Supplementary Fig. 1

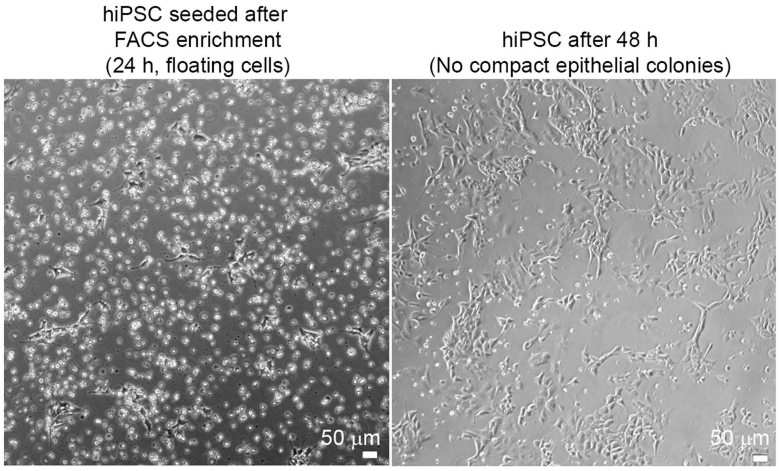

Supplementary Fig. 1. Morphology and survival of human iPSCs. Morphology of flow cytometry-sorted hiPSCs (> 97% TRA-1-60) seeded on Matrigel-coated plates. Single cell dissociation results in loss of colonies and significant cell death.

+

Supplementary Fig. 2

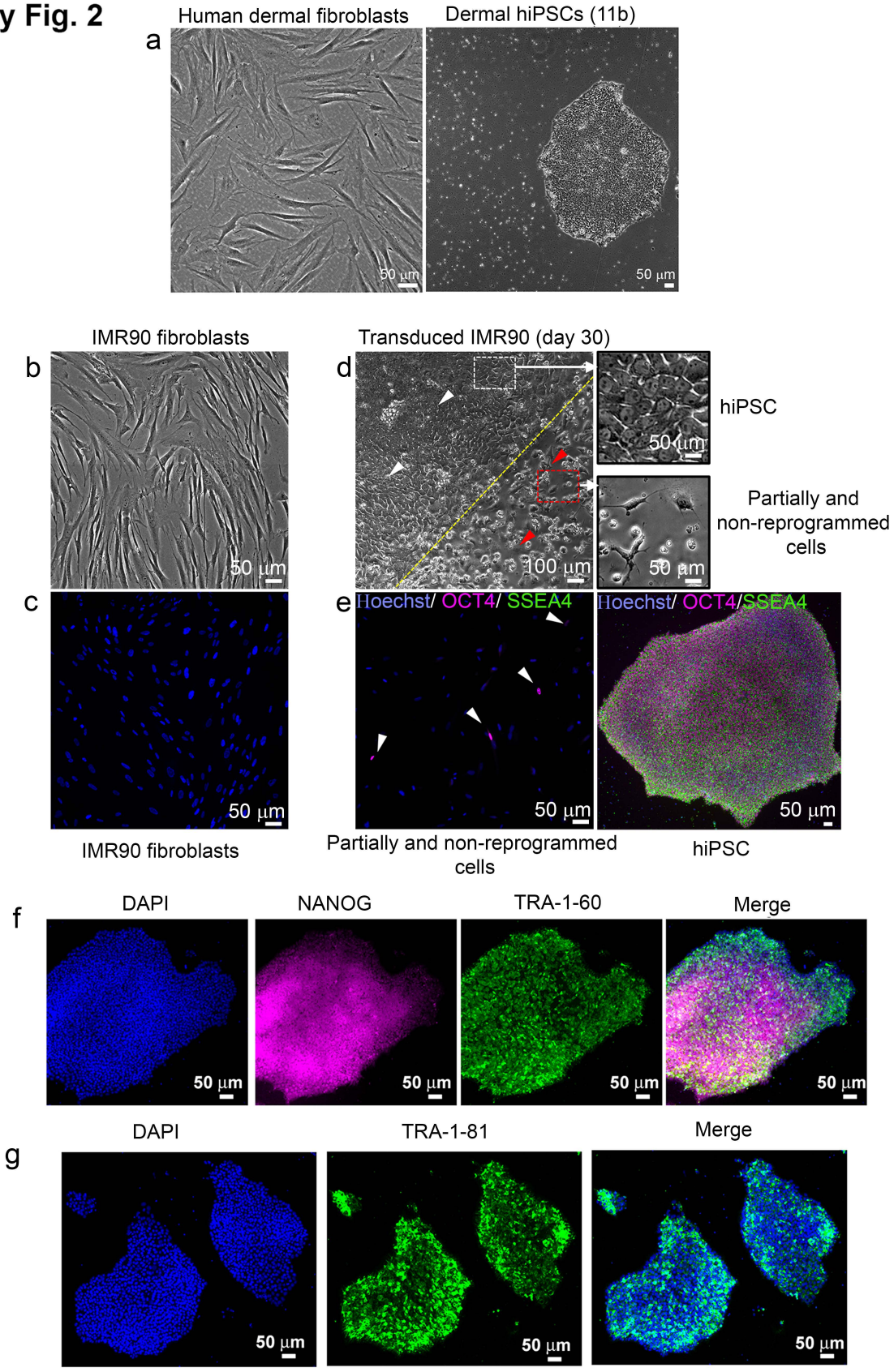

Supplementary Fig. 2. Morphology and pluripotency of reprogrammed hiPSCs. (**a**) Morphology of spread human dermal fibroblasts and epithelial-like hiPSCs. (**b–e**) Morphology and expression of pluripotency markers in parental fibroblast (b,c), and in reprogrammed cultures, 30 days after lentivral transduction (d, left panel in e). Fully reprogrammed (white arrowheads, white box) and non-reprogrammed/partially reprogrammed cells (red arrowheads, red box) are indicated. The right panel in (e) shows a colony from a manually passaged hiPSC line for comparison.(**f–g**) Expression of pluripotency markers TRA-1-60, NANOG, and TRA-1-81 in reprogrammed IMR90-derived hiPSCs.

Supplementary Fig. 3

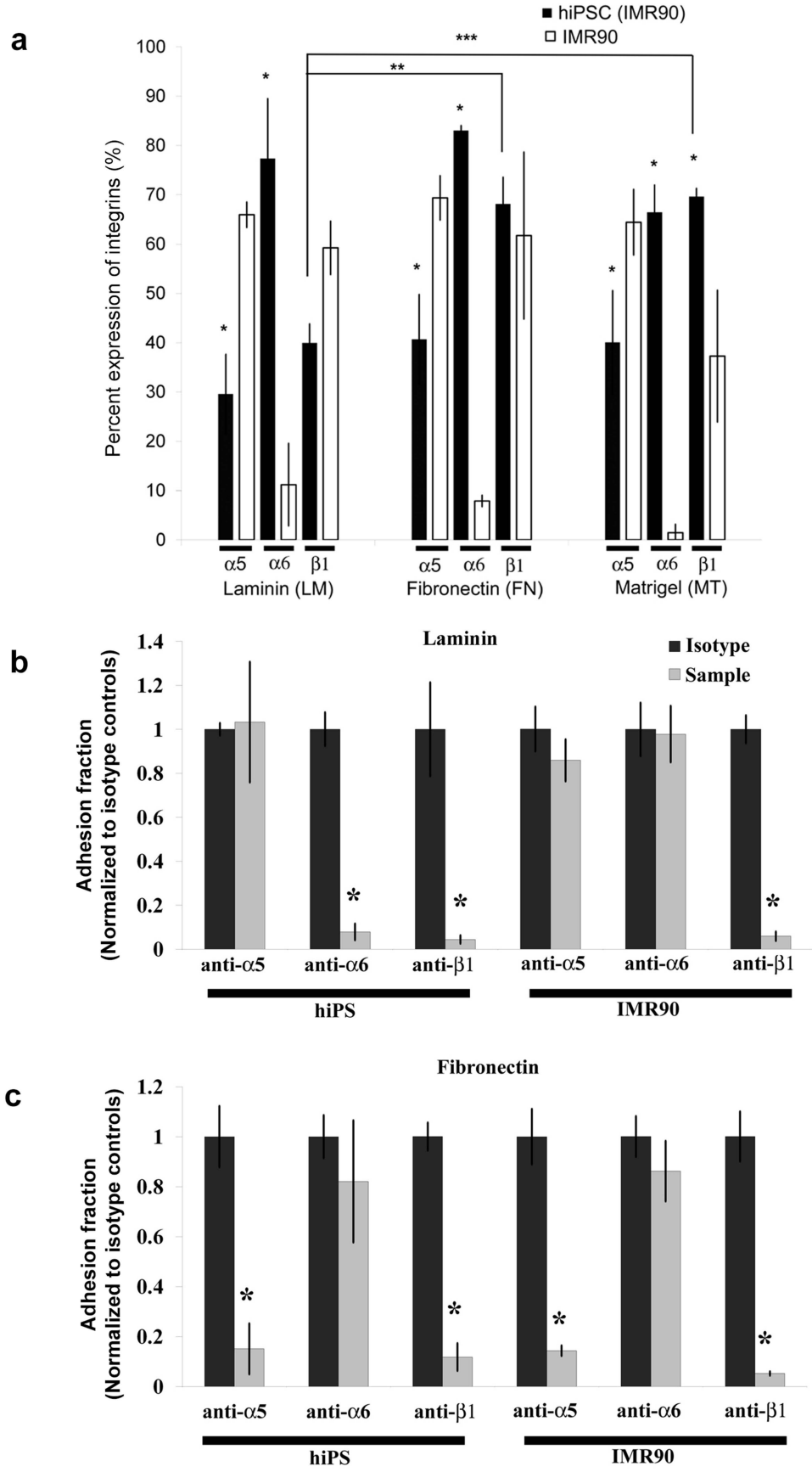

Supplementary Fig. 3. Changes in integrin expression with reprogramming. (**a**) Flow cytometry measurement of integrins expressed on hiPSCs and IMR90 cells cultured on laminin, fibronectin, and Matrigel (**P* < 0.05 hiPSC vs. IMR90, ***P* < 0.05 laminin vs. fibronectin, ****P* < 0.05 laminin vs. Matrigel). Differences in expression of integrins α5, α6, and β1 involved in fibroblast and hiPSC adhesion to fibronectin, laminin, and Matrigel were observed.

Flow cytometry analyses revealed 30–35% higher expression of α5 integrins on IMR90 fibroblasts compared to hiPSCs ($P < 0.05$), regardless of whether the cells were cultured on fibronectin, laminin or Matrigel. In contrast, hiPSCs expressed 60–70% more α6 integrins than IMR90 cells for all matrices. The expression of β1 subunit by hiPSCs was significantly higher only when cultured on Matrigel compared to IMR90 cells. (b,c) Blocking of integrin-mediated adhesion to laminin and fibronectin using integrin-specific blocking antibodies (*$P < 0.05$ blocking antibody vs. isotype) revealed that β1 integrin was critical for IMR90 and hiPSC adhesion to these matrices. Blocking α6 integrin significantly reduced hiPSC adhesion to laminin but did not inhibit the adhesion of IMR90 cells. Blocking α5 integrins significantly reduced the adhesion of hiPSCs and IMR90 cells to fibronectin but it did not alter adhesion to laminin. Bar graph represents average ± S.D (n = 3).

Supplementary Fig. 4

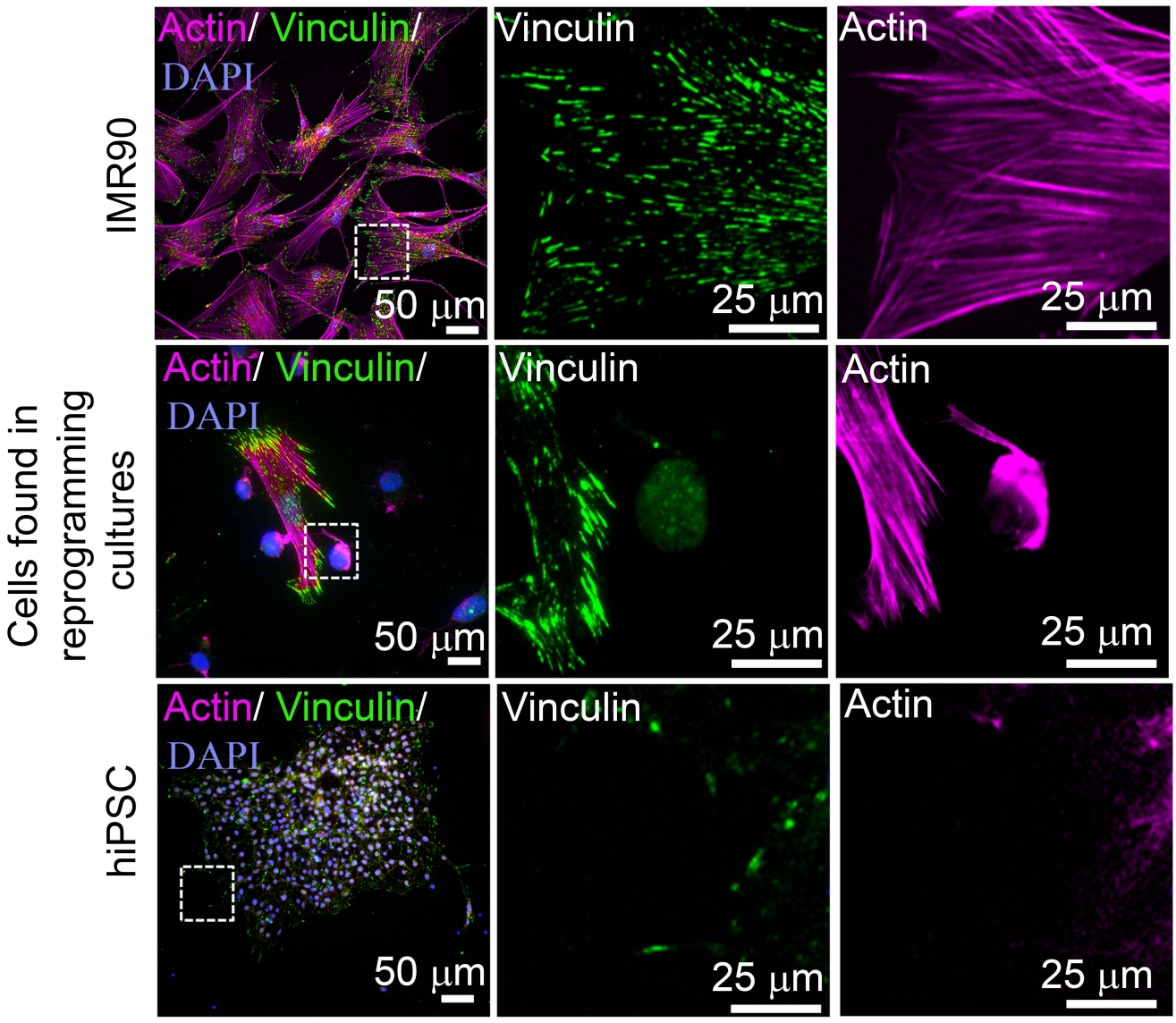

Supplementary Fig. 4. Immunostaining for actin and vinculin in the indicated cell types, cultured on laminin .

Supplementary Fig. 5

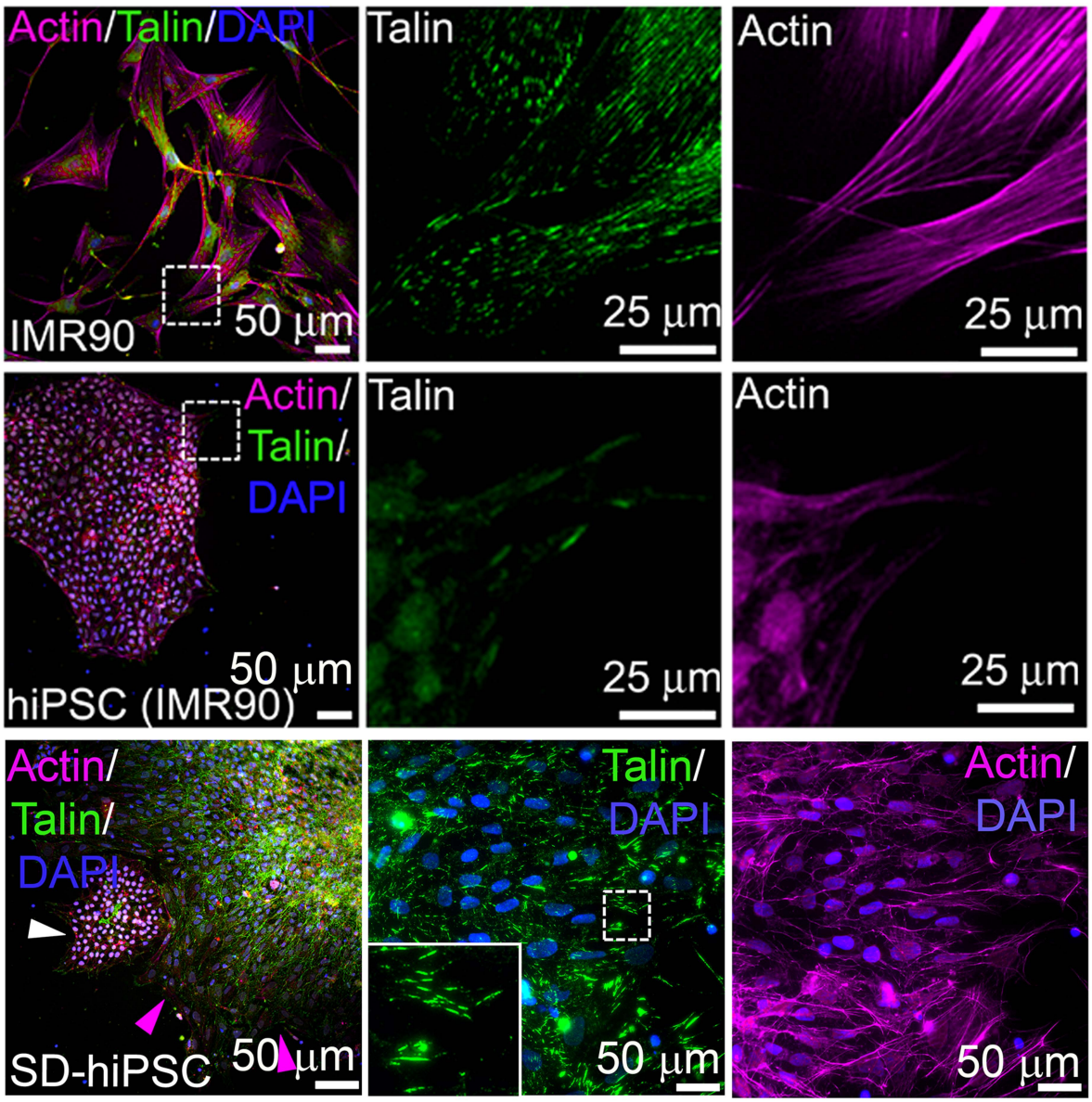

Supplementary Fig. 5. Immunostaining for actin and talin in the indicated cell types, cultured on laminin .

Supplementray Fig. 6

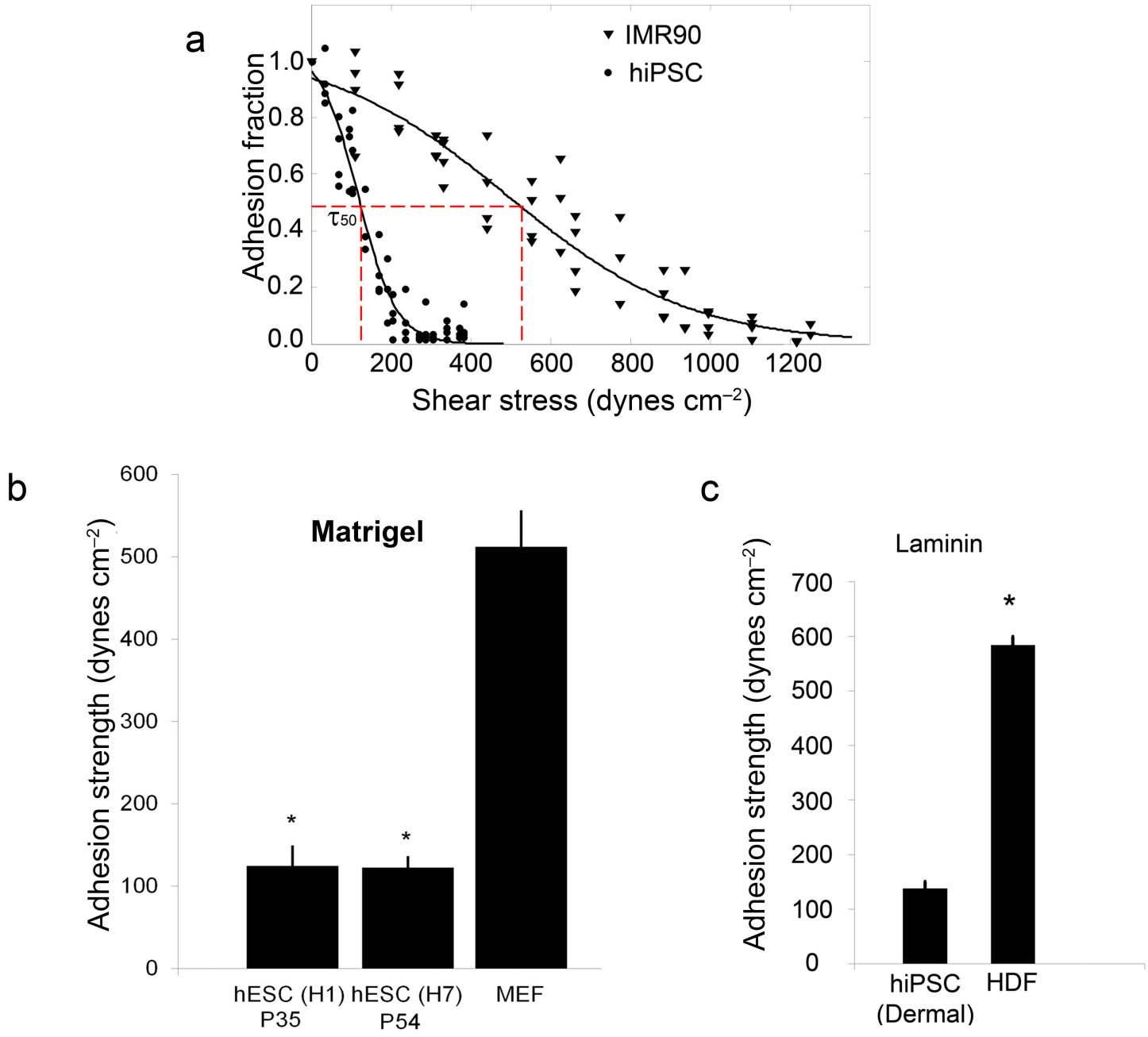

Supplementary Fig. 6. Adhesion strength analysis of hPSCs. (**a**) Detachment profile showing adherent cell cluster fraction vs. applied shear stress for hiPSCs and IMR90 cells. Experimental points were fit to sigmoid to obtain the shear stress for 50% detachment τ50. The significant left-ward shift in the sigmoidal profile for hiPSCs compared to IMR90 cells indicates a reduction in the adhesion strength for reprogrammed hiPSCs. (**b**) Adhesion strength for hESCs (H7 and H1) compared to MEF on Matrigel. Bar graph shows average ± S.D. (*P < 0.05 stem cells vs. MEF). (**c**) Adhesion strength for hiPSCs (derived from dermal fibroblasts) and human dermal fibroblasts on laminin. Bar graph represents average ± S.D. (*P < 0.05 stem cells vs. fibroblasts).

Supplementary Fig. 7

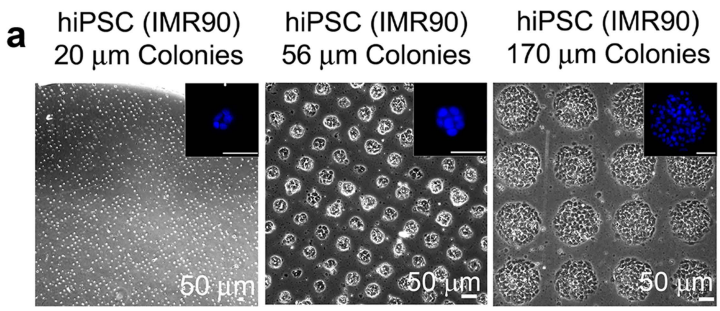

b

Island diameter	hiPSC colony area	Average cell count
20 μm	314 μm^2	4 ± 1
56 μm	2463 μm^2	8 ± 2
170 μm	22700 μm^2	70 ± 10

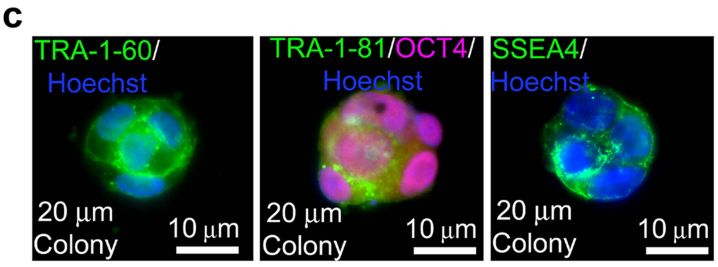

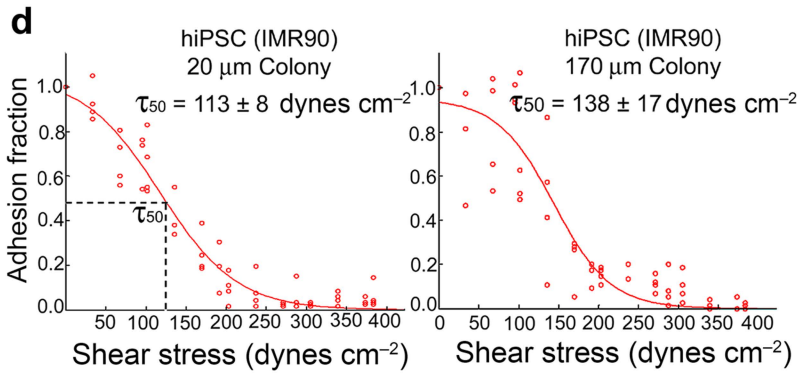

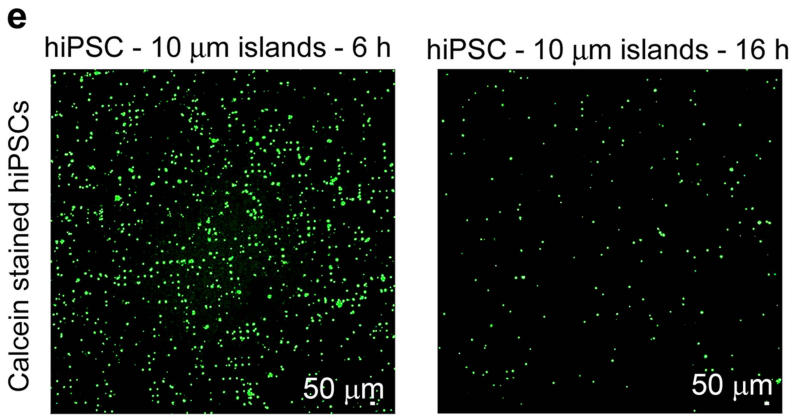

Supplementary Fig. 7. Role of colony size on hiPSC adhesion strength. Arrays of circular adhesive islands of varying dimensions (10, 20, 56, and 170 μm dia.) were engineered to examine a nearly 100-fold range in available adhesive area (**a**) Phase contrast images of micropatterned hiPSC clusters on 20, 56, and 170 μm diameter fibronectin adhesive islands. Inset shows a single cell cluster with DAPI-stained nuclei. (**b**) Table presenting number of hiPSCs adhering to 20, 56, and 170 μm islands of fibronectin. (**c**) Immunostained images showing undifferentiated state of hiPSCs stained for OCT4, SSEA4, TRA-1-60, TRA-1-81 on micropatterned substrates. (**d**) Detachment profile showing adherent cell cluster fraction vs. applied shear stress for hiPSCs on 20 and 170 μm diameter islands. (**e**) Micropatterned hiPSCs on 10 μm size adhesive islands of fibronectin. Whereas on the larger islands, hiPSCs colonies adhered well and exhibited high (> 95%) viability, hiPSCs adhered loosely as individual cells on 10 μm adhesive islands and did not survive in overnight culture (green, live cells).

Supplementary Fig. 8

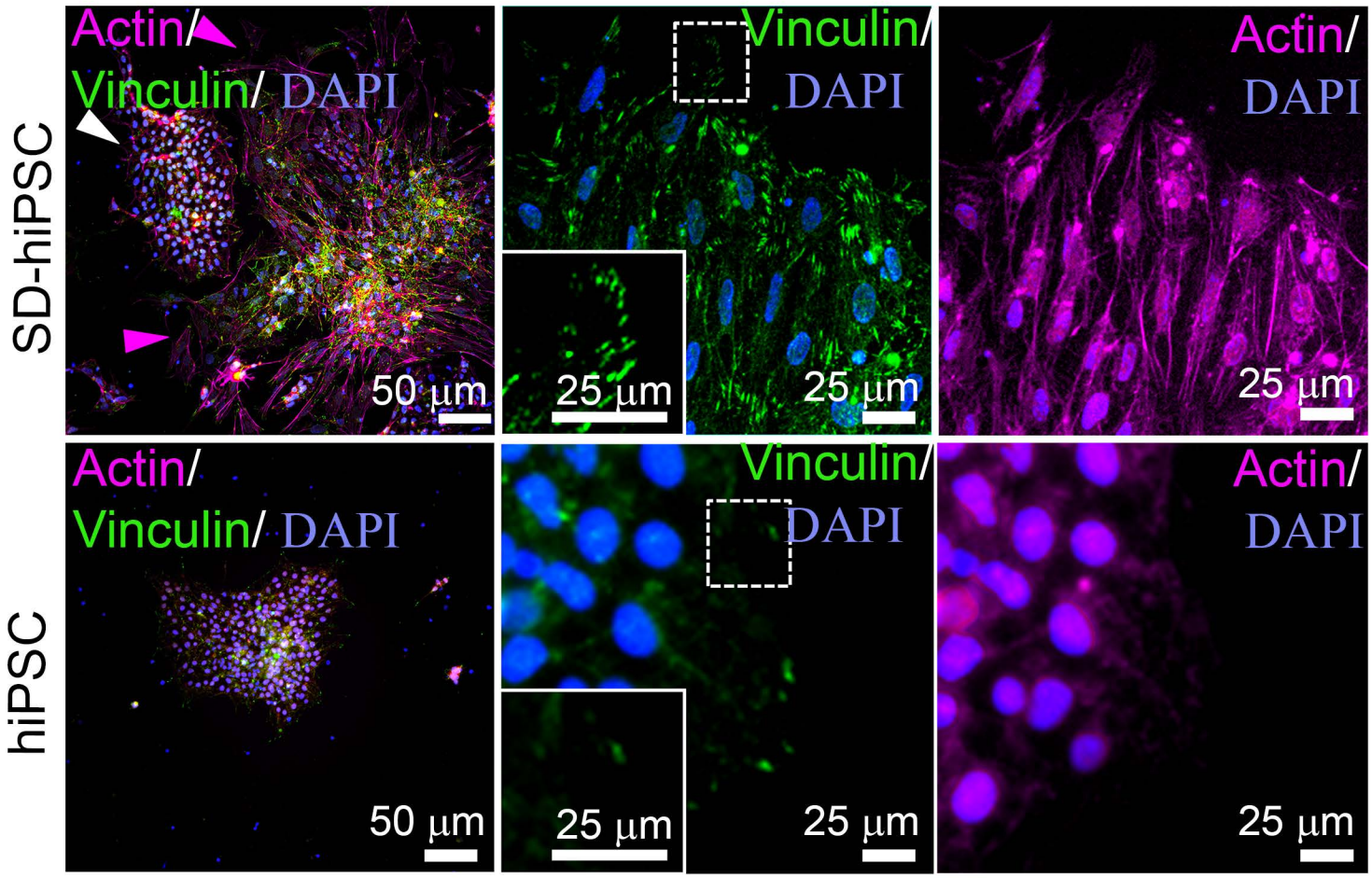

Supplementary Fig. 8. Immunostaining for the indicated markers in hiPSCs and in spontaneously differentiating (SD) cultures of hiPSCs. Magenta arrowheads show recruitment of vinculin to focal adhesions in SD cultures, distinct from hiPSCs (white arrowhead).

Supplementary Fig. 9

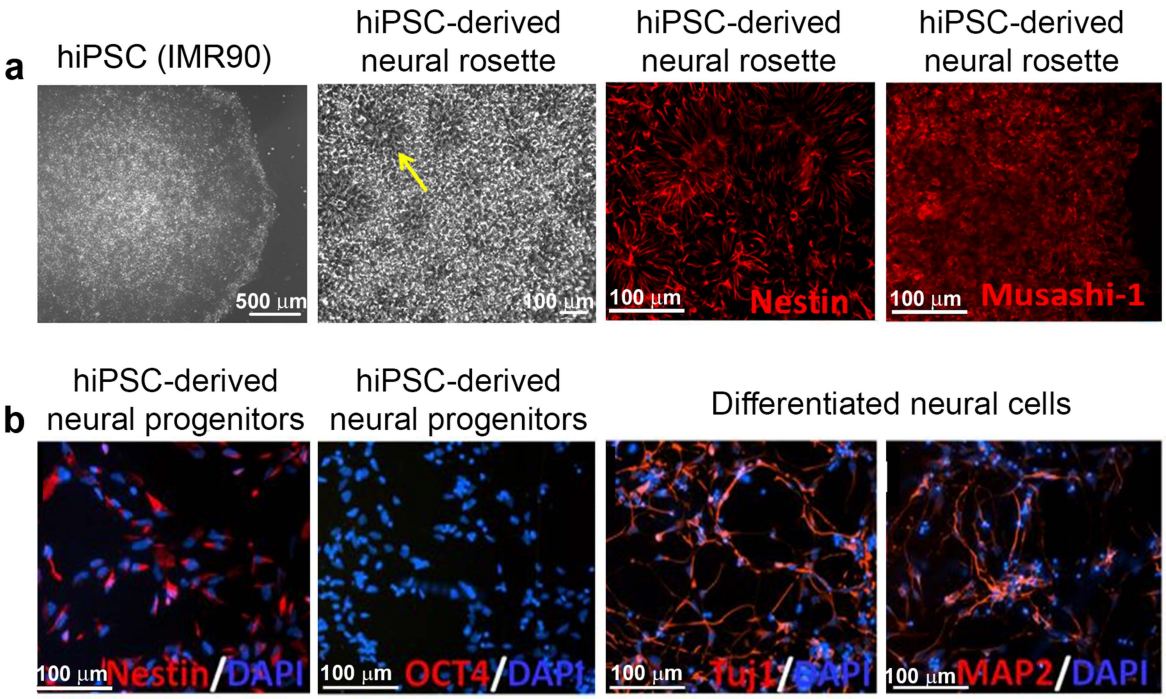

Supplementary Fig. 9. Expression markers and morphology of neural stem cells. (**a**) hiPSC-derived neural rosettes and (**b**) hiPSC-derived neural progenitors and their differentiation to neural lineages (Tuj1 and MAP2).

Supplementary Fig. 10

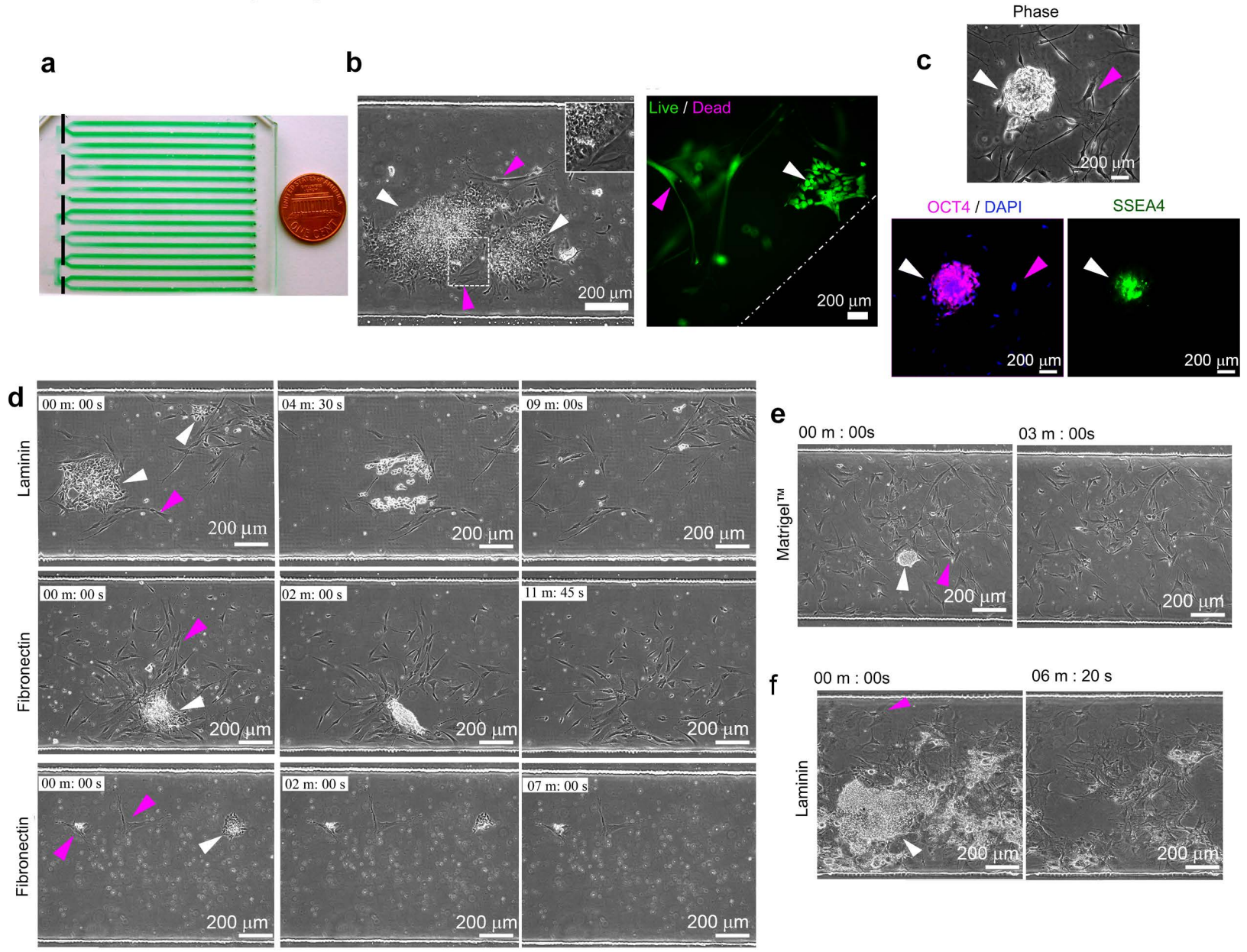

Supplementary Fig. 10. Stem cell surival and detachment in µSHEAR. (**a)** 16-channel µSHEAR (area corresponding to a 6-well plate), with cells typically adhered in the green-dye area. (**b**) hiPSCs (white arrowheads, compact epithelial colonies) and IMR90 cells (red arrowheads, elongated cells) cocultured in microfluidic channel. Live and dead staining for viable hiPSCs (white arrowhead) and IMR90 cells (red arrowhead). Live cells stained green for calcein-AM while dead cells stain red for ethidium homodimer. (**c**) hiPSCs (overnight culture) remain undifferentiated in microfluidic devices as stained positive for OCT4 and SSEA4. (**d,e**) Selective detachment of hiPSC colony (white arrow) from laminin, fibronectin, and Matrigel. Colonies were selectively detached at a shear stress of 85–125 dynes cm^{-2} (**f)** Selective detachment of hESC colony from laminin in the presence of MEF (red arrow).

Supplementary Fig. 11

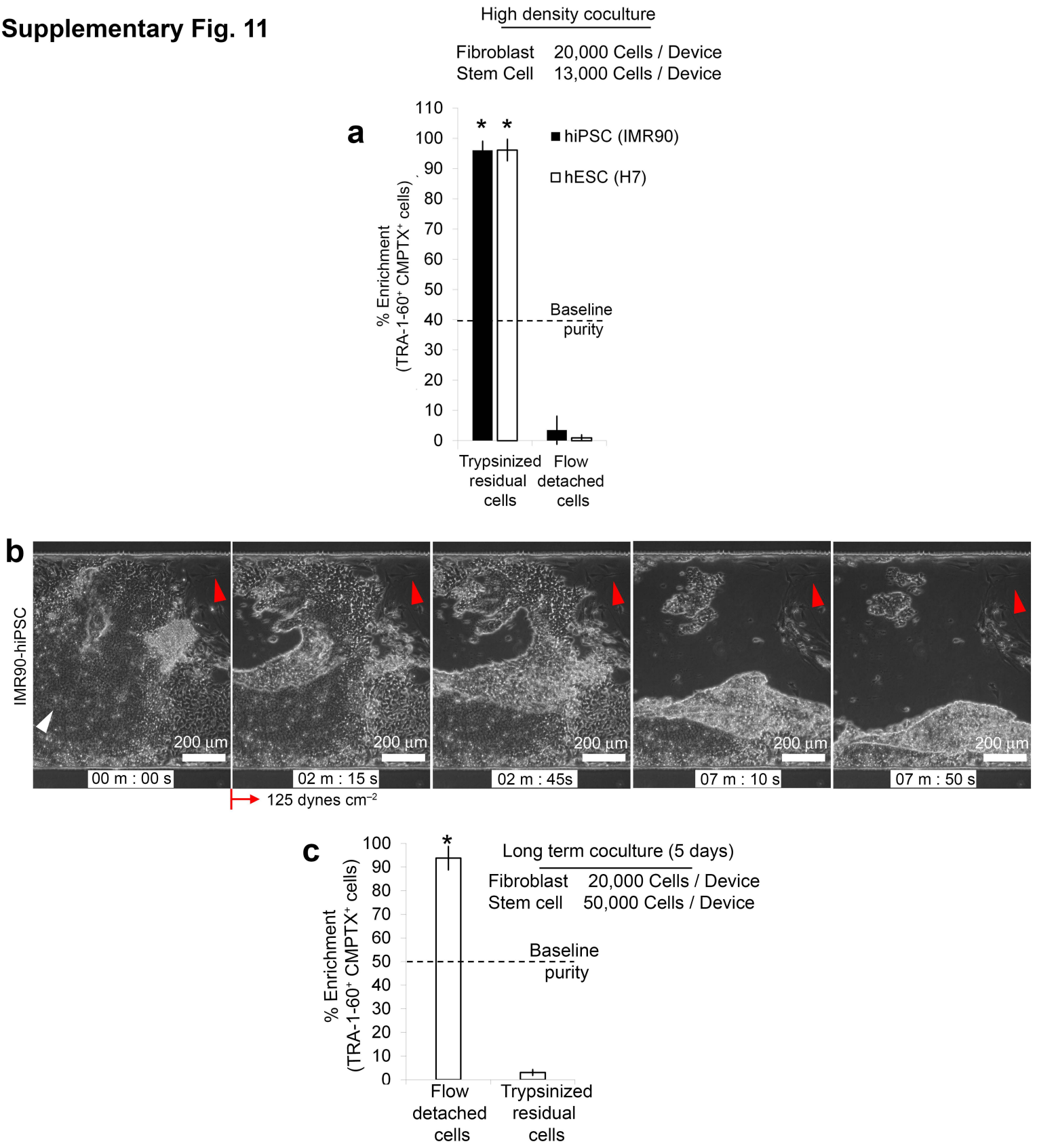

Supplementary Fig. 11. Flow cytometry-based measurements of enrichment of hiPSCs. (**a**) Bar graph presenting flow cytometry-based measurements of enrichment of hiPSCs and hESCs (H7) isolated at 85–125 dynes cm^{-2} from a coculture of IMR90 and MEF cells, respectively. Figures also display residual stem cells in the devices post µSHEAR-based isolation. (**b**) Selective isolation of hiPSC colonies after 5 days of coculture with IMR90 fibroblasts on laminin and (**c**) enrichment of hiPSCs detached at 85–125 dynes cm^{-2} from 5-7 day cultures.

Supplementary Figure 12

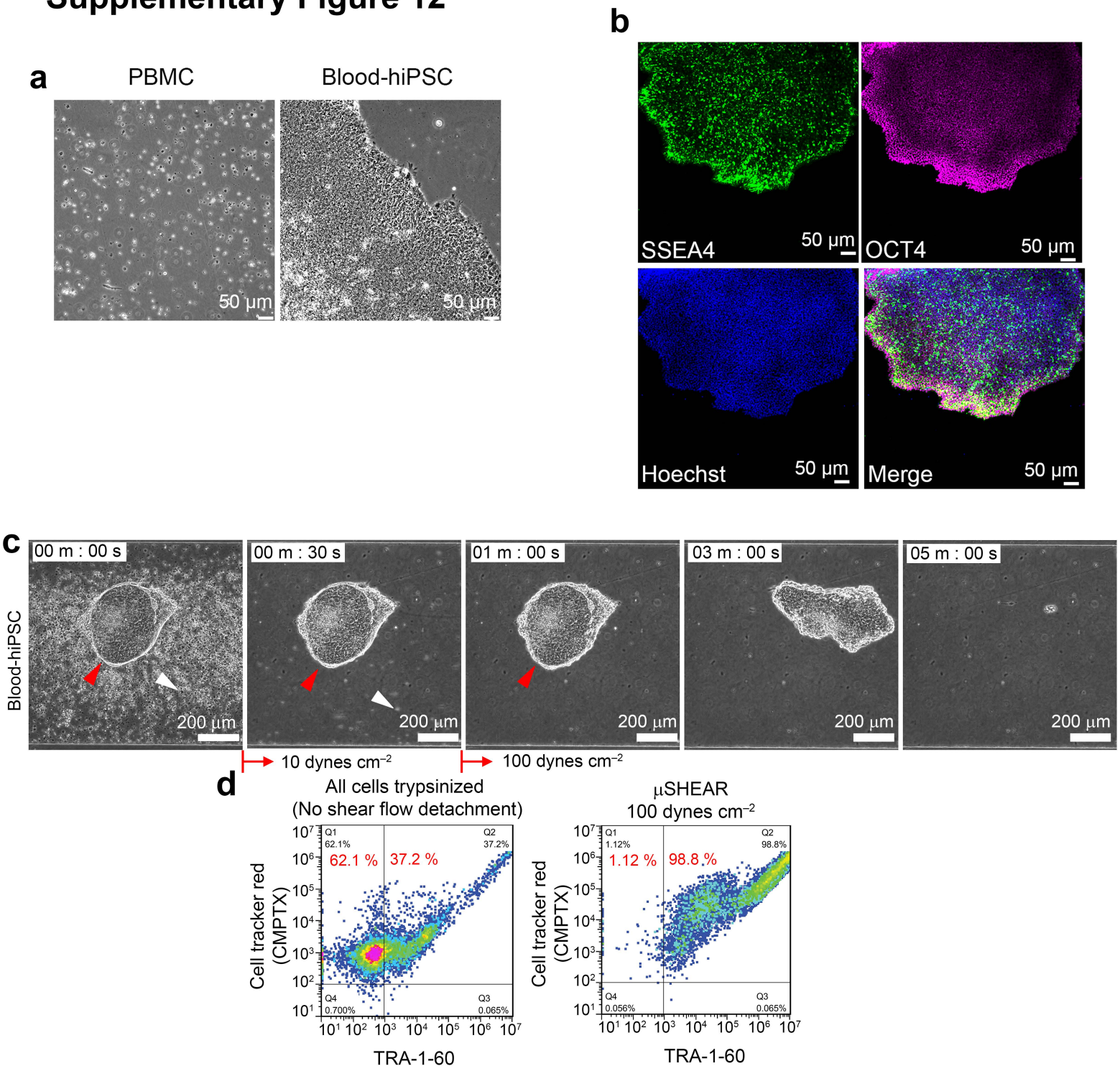

Supplementary Fig. 12. Characterization and isolation of blood cell-derived hiPSCs. (**a**) Morphology of loosely adhesive or non-adhesive human peripheral blood mononuclear cells (PBMC) and epithelial-like blood cell-derived hiPSCs. (**b**) Pluripotency markers TRA-1-60, NANOG, and TRA-1-81 expressed by reprogrammed PBMC-derived hiPSCs. (**c**) Isolation of PBMC-derived hiPSCs cocultured with PBMCs. Loosely adherent PBMCs were removed at 10 dynes cm^{-2} and hiPSCs were harvested by increasing the flow to 100 dynes cm^{-2}. (**d**) Flow cytometry measurements of enrichment of blood cell-derived hiPSCs detached at 100 dynes cm^{-2}.

Supplementary Flg. 13

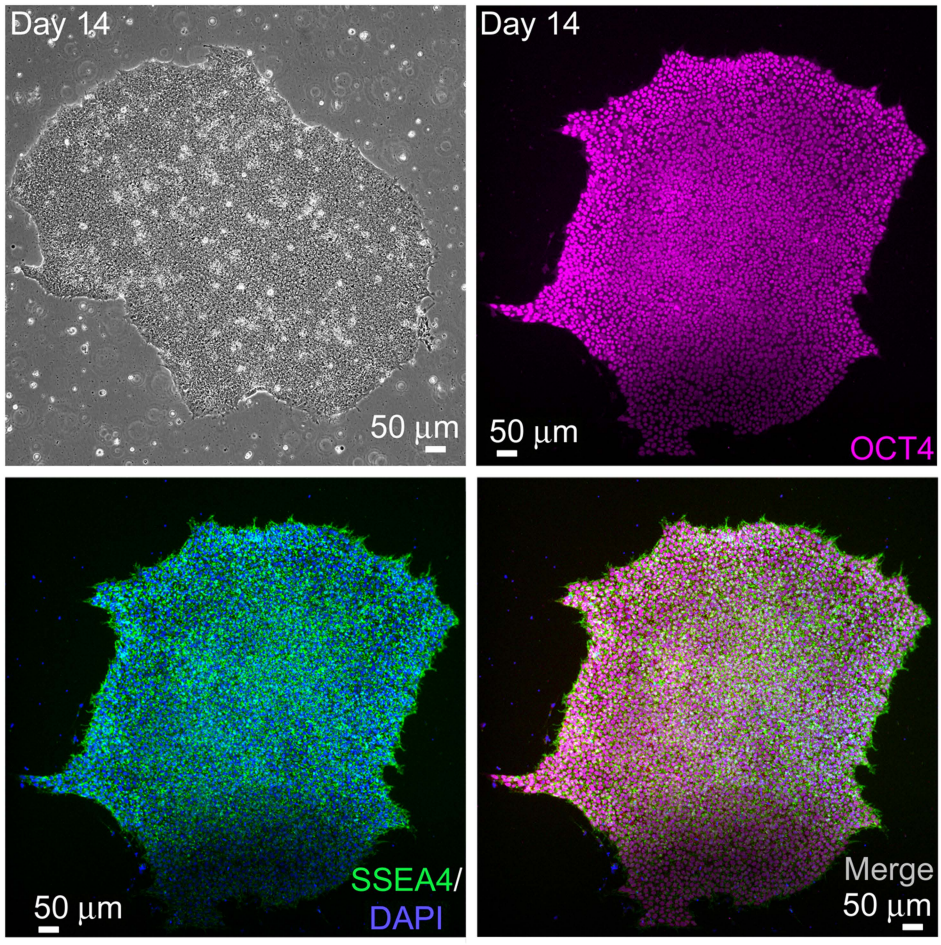

Supplementary Fig. 13. Detached hiPSC colonies cultured on Matrigel adhere as colonies. Immunofluorescence staining for pluripotency markers SSEA4 and OCT4 showing detached and recovered hiPSC colonies cultured on Matrigel retained undifferentiated characteristics (day 14).

Supplementary Fig. 14

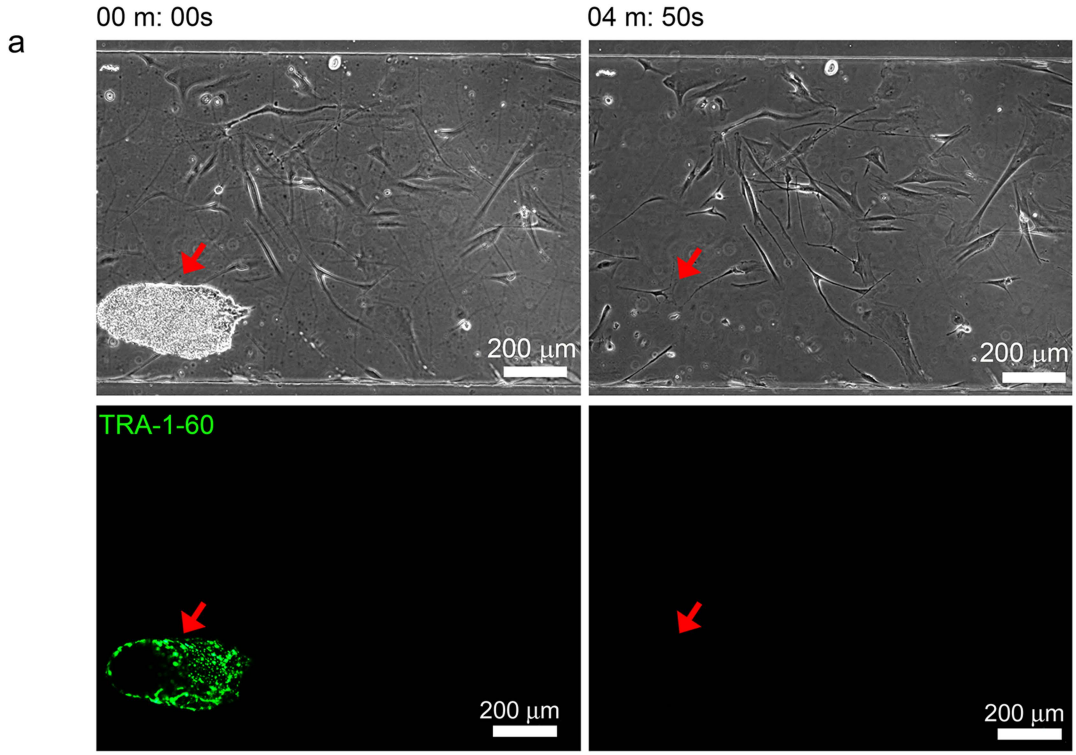

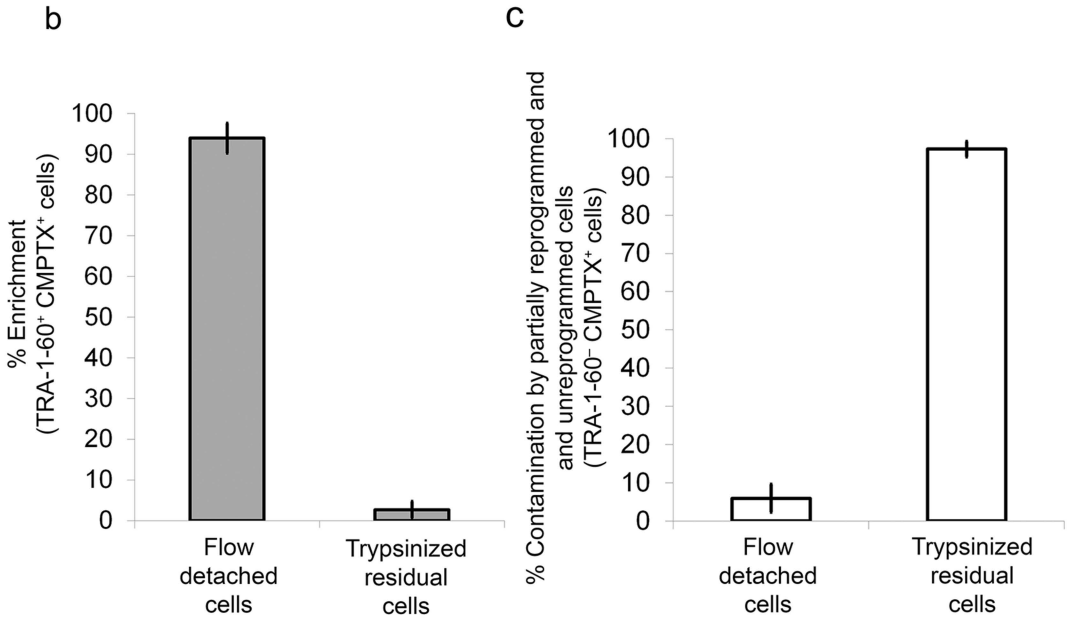

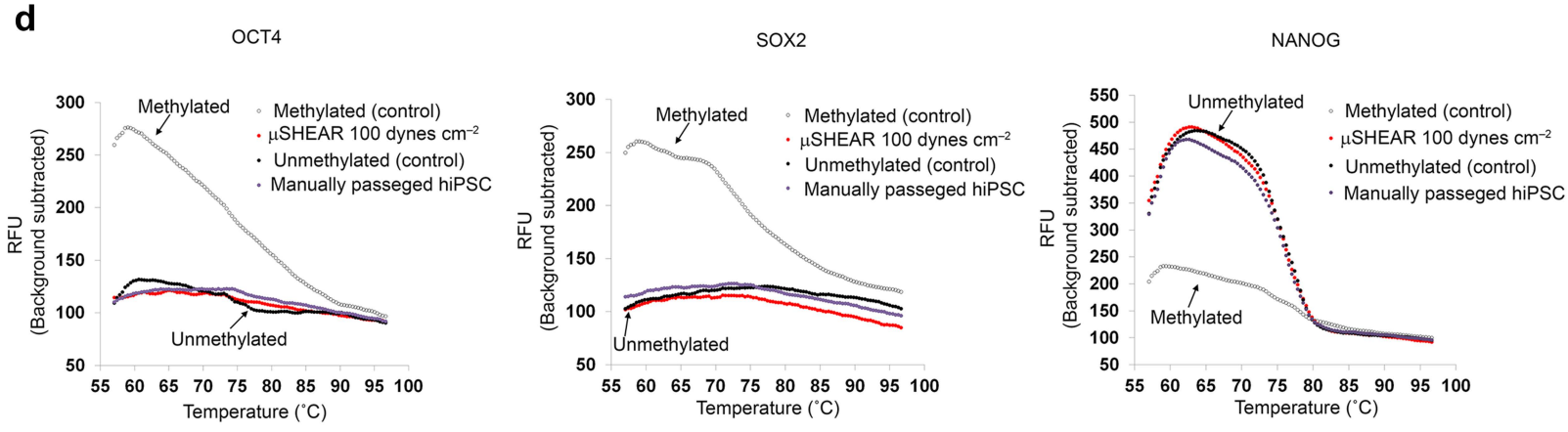

Supplementary Fig. 14. μSHEAR-based isolation of hiPSCs from a heterogeneous reprogramming culture. (**a**) Reprogrammed hiPSCs (TRA-1-60 positive) and partially reprogrammed untransduced cells (TRA-1-60 negative) in microfluidic channel. Colonies of hiPSCs were selectively detached at 100 dynes cm^{-2} shear stress. (**b**) Bar graph presenting flow cytometry-based measurements of enrichment of hiPSCs isolated at 100 dynes cm^{-2} from a heterogeneous reprogramming culture. Figure also represents residual hiPSCs in the devices post μSHEAR-based isolation. (**c**) Bar graph presents flow cytometry measurements of contamination of partially reprogrammed and untransduced cells in cells isolated by μSHEAR vs. trypsinization. (**c**) Methylation patterns for OCT4, SOX2, and NANOG promoters using bisulfite sequencing based melting curve analysis of PCR products. Curves with open circles represented 100% methylated DNA controls and curves with closed black circles represent unmethylated DNA controls. Bar graph shows average ± S.D. (*$P < 0.05$)

Supplementary Fig. 15

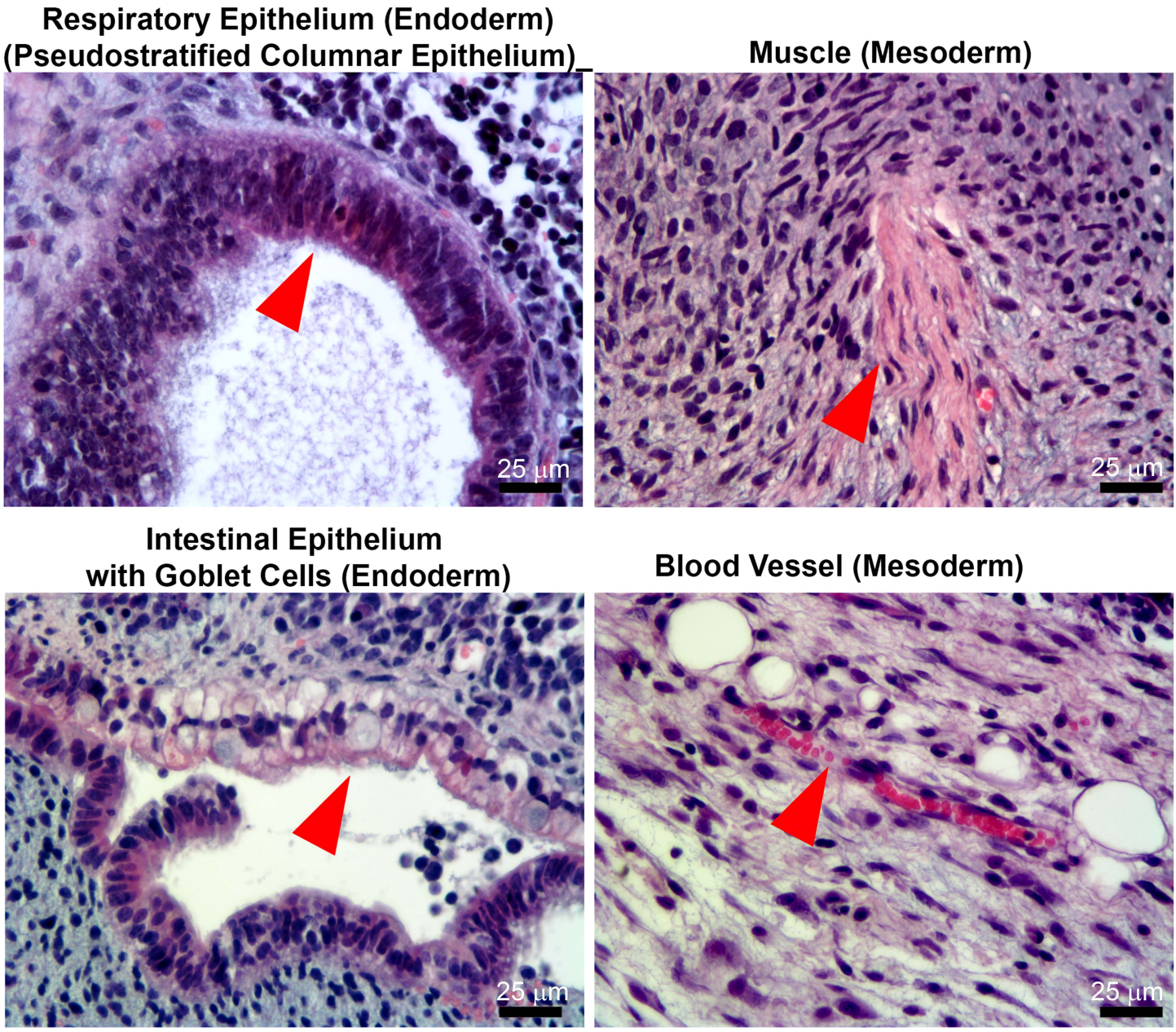

Supplementary Fig. 15. Higher magnification of hematoxylin-eosin (H/E) stained sections from a formalin-fixed teratoma produced by µSHEAR-isolated hiPSCs.

Supplementary Fig. 16

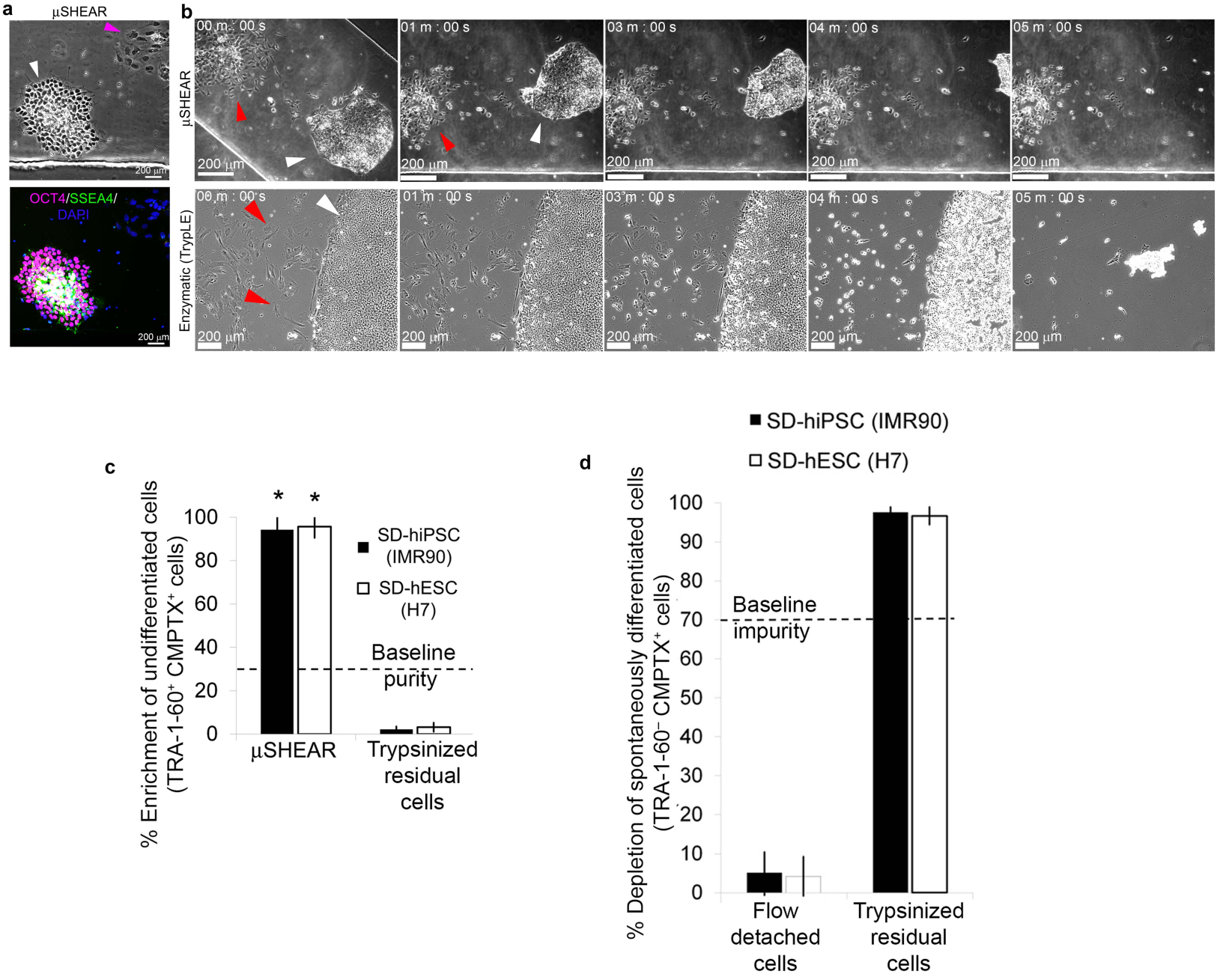

Supplementary Fig. 16. Enrichment efficiency of spontaneously differentiated cultures (SD) of hiPSCs.

(**a**) Immunostaining for OCT4 (red) and SSEA4 (green) indicating undifferentiated cells (white arrowhead) while negative expression corresponds to differentiated (red arrowhead) hiPSCs cultured in µSHEAR device. (a) Micrographs show µSHEAR-based isolation of hiPSCs (white arrowhead) from spontaneously differentiating cells (red arrowhead) at 100 dynes cm^{-2} Bottom panel shows enzymatic detachment of cells. (**c**) Bar graph presents flow cytometry measurements for enrichment of hiPSCs and hESC (H7) isolated at 85–150 dynes cm^{-2} from a spontaneously differentiated culture using µSHEAR. Plot also shows residual undifferentiated stem cells in devices after µSHEAR-based isolation. (**d**) Flow cytometry results showing isolated hiPSCs (positive for TRA-1-60 and CMPTX) and SD-hiPSCs (positive for CMPTX only). Bar graph shows flow cytometry measurements of contamination of SD-hiPSCs and SD-hESC (H7) in recovered cells selectively isolated at a shear stress of 85–125 dynes cm^{-2}

Supplementary Fig. 17

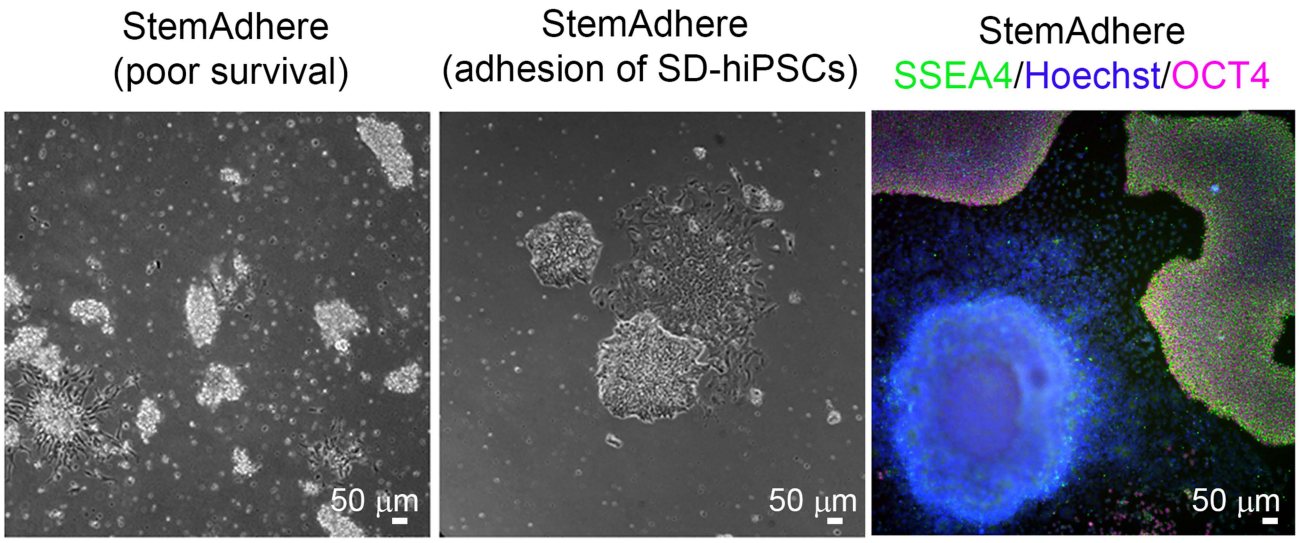

Supplementary Fig. 17. Spontaneously differentiated (< 10%) hiPSCs cultured on StemAdhere. Seeded colonies exhibited poor survival (floating colonies, left), with adhesion of differentiated cells along-with undifferentiated cells (middle, right). Differentiated cells did not express pluripotency markers OCT4 and SSEA4.

Supplementary Fig. 18

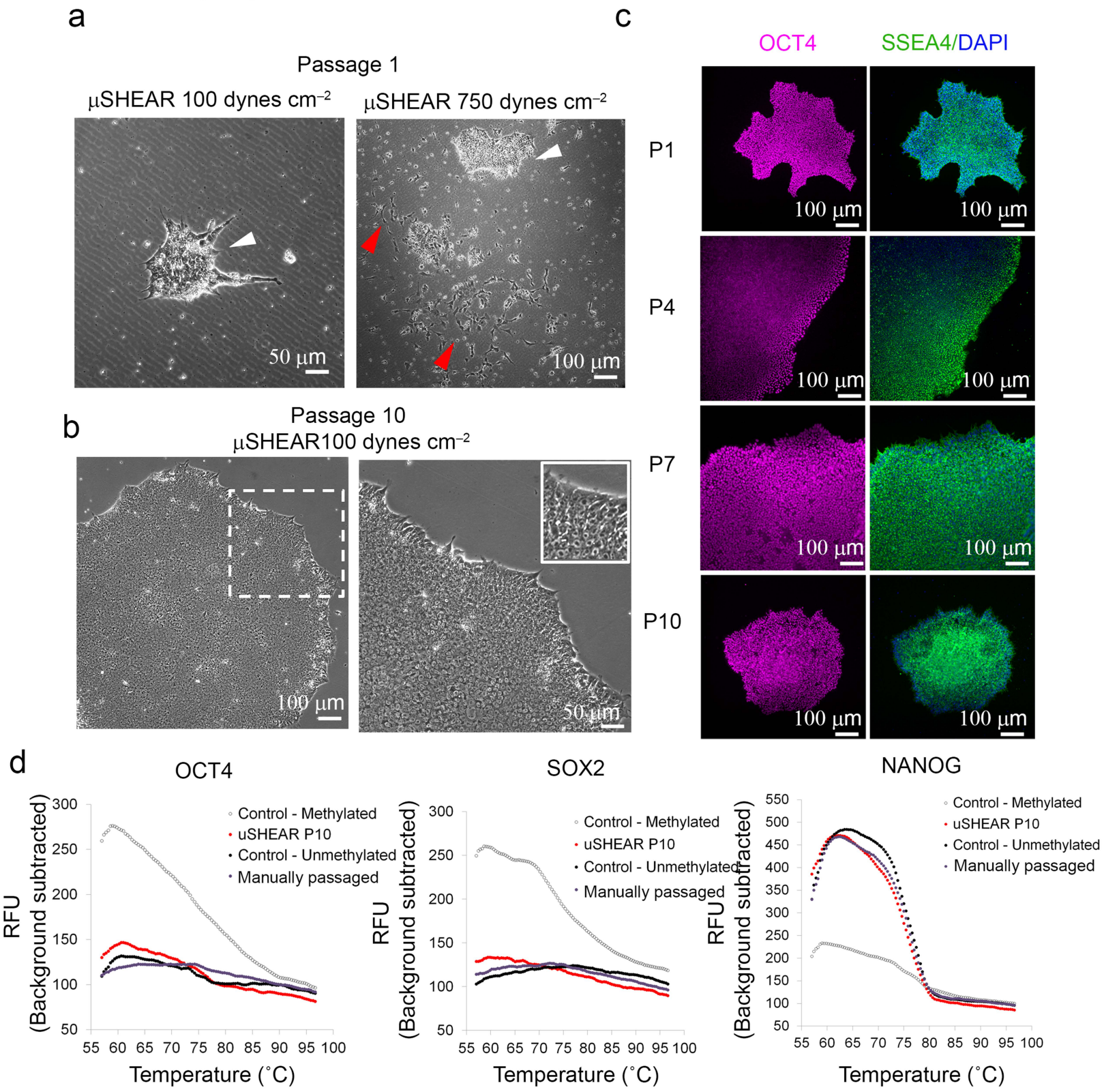

Supplementary Fig. 18. Characteristics of μSHEAR-isolated colonies cultured on Matrigel. (a) μSHEAR-isolated colonies cultured on Matrigel adhere as undifferentiated colonies (100 dynes cm^{-2} day 2, white arrows) or partially differentiated colonies (750 dynes cm^{-2} day 2, red arrows). (b) hiPSC colonies exposed to repeated 10 device-based passages retained high nucleus to cytoplasm ratio and self-renewal properties indicated by colony expansion when cultured on Matrigel. (c) Immunofluorescence staining for pluripotency markers SSEA4 and OCT4 showing detached hiPSC colonies cultured on Matrigel retained stemness for at least 10 passages using μSHEAR. (d) Methylation patterns for OCT4, SOX2, and NANOG promoters using bisulfite sequencing based melting curve analysis of the PCR products. Curves with open circles represented 100% methylated DNA controls and curves with closed black circles represent unmethylated DNA controls.

Supplementary Fig. 19

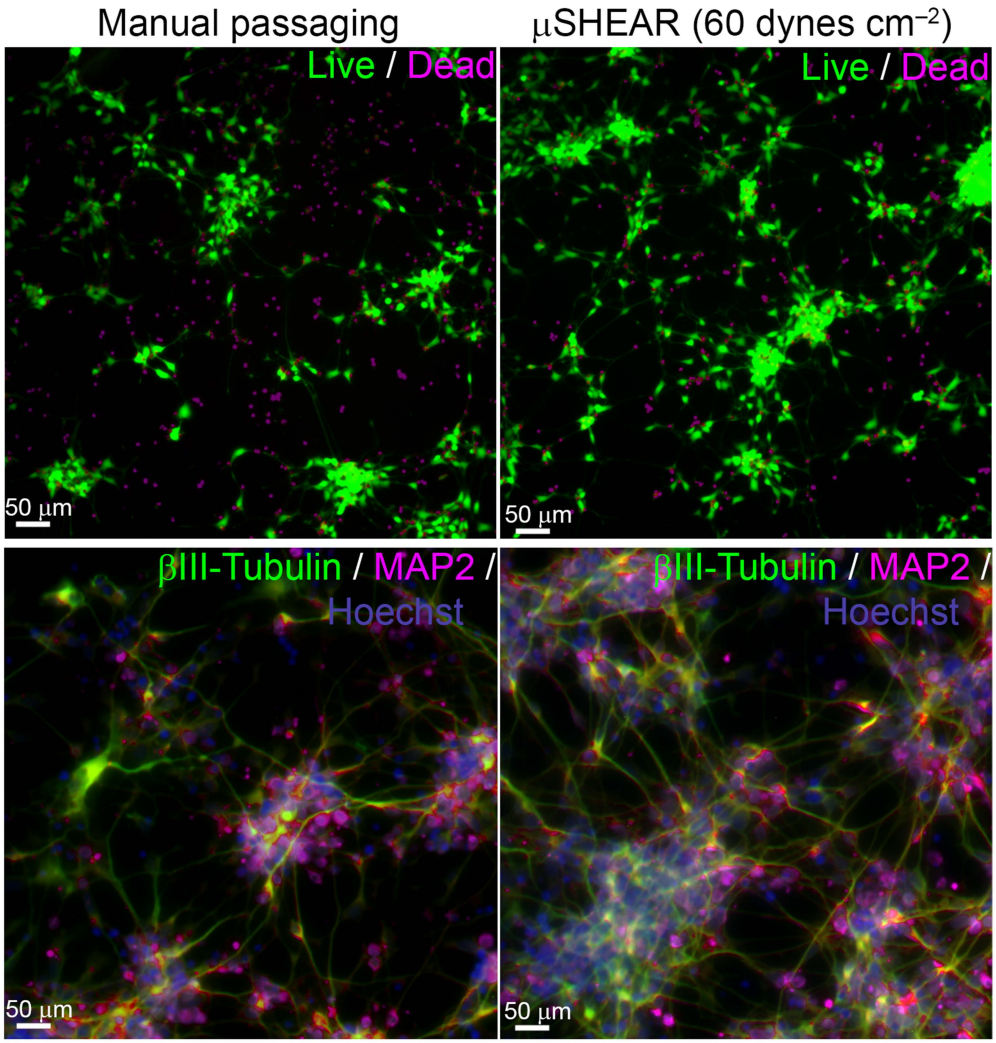

Supplementary Fig. 19. Microfluidic cell separation does not adversely affect isolated neural cells. 24 h post microfluidic and manual passage, microfluidic neuron cultures (right) are not adversely affected compared to manually passaged neuron cultures (left). (Top) Number of viable cells; (Bottom) Replated cells have normal neurite outgrowth and β-III tubulin and MAP2 expression.

Supplementary Fig. 20

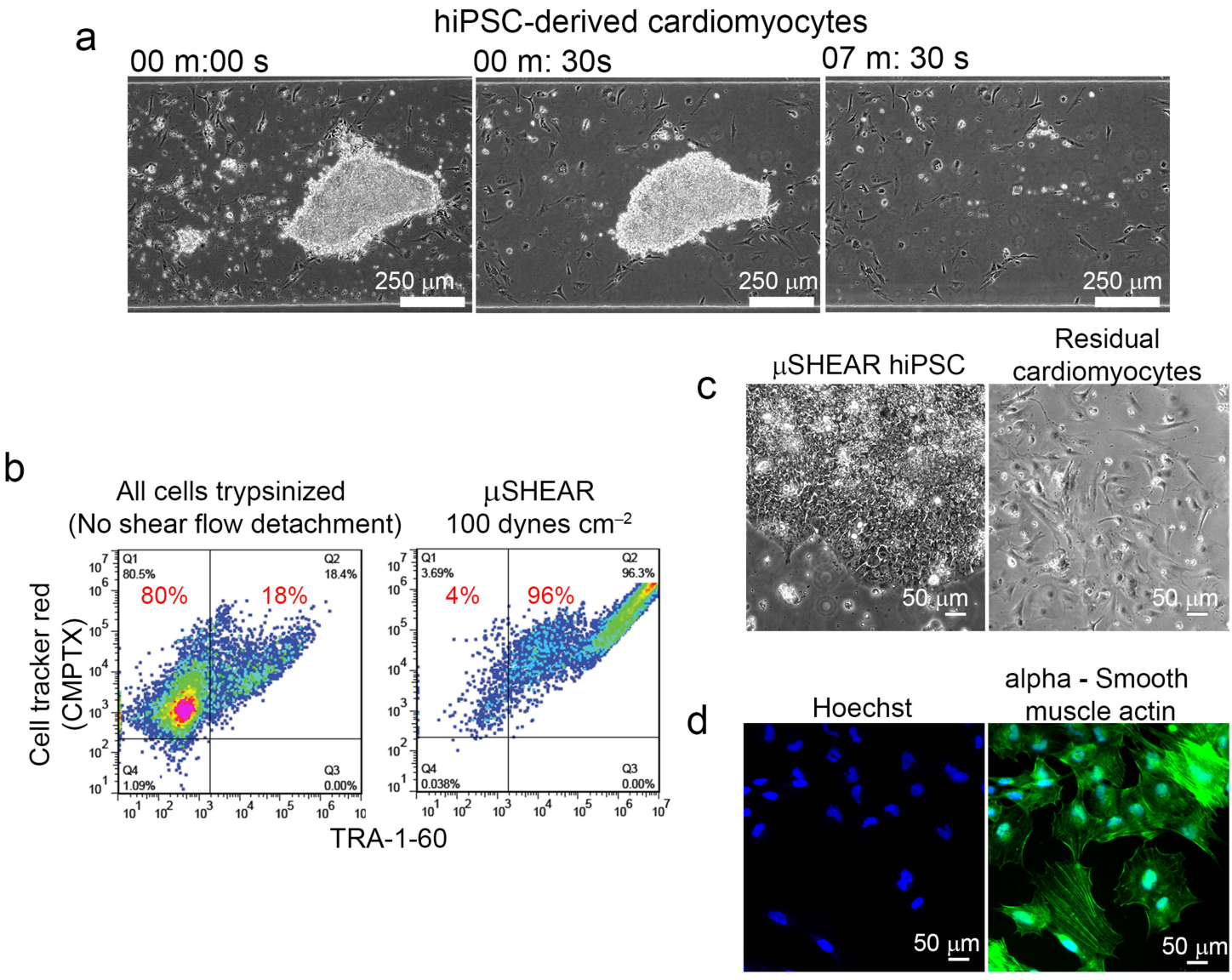

Supplementary Fig. 20. Selective detachment of hiPSC (IMR90) colonies cocultured with high density hiPSC(IMR90)-derived cardiomyocytes. (**a**) hiPSCs were harvested at 100 dynes cm^{-2}.(**b**) Flow cytometry measurements of enrichment of hiPSCs detached at 100 dynes cm^{-2}. (**c**) Detached hiPSC colonies cultured on Matrigel adhere as colonies. (**d**) Trypsinized residual cardiomyocytes adhere and proliferate on Matrigel and stained positive for α-smooth muscle actin.

Supplementary Table 1. Primary and secondary antibodies used in the study.

Marker	Primary Antibody	Secondary Antibody (Dilution 1:200.)
OCT3/4	Rabbit Oct-3/4 (H-134): sc-9081(Santa Cruz Biotechnology). Dilution 1:200.	Alexa Fluor 546-IgG (Life Technologies)
SSEA4	Mouse MC-813-70 (SSEA-4) (Developmental Studies Hybridoma Bank). Dilution 1:25.	Alexa Fluor 488-IgG (Life Technologies)
Integrin β1	Mouse anti-human integrin beta1 monoclonal antibody, clone P4G11, (MAB1951Z, Millipore). Dilution 1:200.	Alexa Fluor 488-IgG
Integrin α5	Mouse anti-human integrin alpha5 monoclonal antibody, (MAB 1956Z, Millipore). Dilution 1:200.	Alexa Fluor 488-IgG
Integrin α6	Rat anti-human integrin alpha6 monoclonal antibody (MAB1378, Millipore). Dilution 1:200.	Alexa Fluor 488-IgG
Integrin β1 (Blocking)	Rat integrin beta-1 (AIIB2, Developmental Studies Hybridoma Bank). Concentration 10 μM.	N/A
TRA-1-81	Mouse monoclonal antibody TRA-1-81 (ab16289, Abcam). Dilution 1:200.	Alexa Fluor 488 or 546-IgG
TRA-1-60	Mouse monoclonal antibody TRA-1-60 (ab16288, Abcam). Dilution 1:200.	Alexa Fluor 488 or 546-IgG
PAX6	Rabbit polyclonal antibody PAX6 (ab5790, Abcam). Dilution 1:200.	Alexa Fluor 488-IgG
α-fetoprotein	Rabbit polyclonal antibody AFP (A0008, Dako). Dilution 1:200.	Alexa Fluor 488-IgG
α-SMA	Rabit polyclonal antibody α-SMA (ab5694, Abcam). Dilution 1:200.	Alexa Fluor 488-IgG
StainAlive™ Mouse Anti-Human TRA-1-60	Stemgent. Dilution 1:200.	DyLight 488 Conjugated
Dnmt3b [52A1018]	Mouse monoclonal antibody Dnmt3b (ab13604, Abcam). Dilution 1:200.	Alexa Fluor 488-IgG
Rex1	Rabbit polyclonal antibody Rex1 (ab50828, Abcam). Dilution 1:200.	Alexa Fluor 546-IgG
GDF3	Rabbit polyclonal antibody GDF3 (ab38547, Abcam). Dilution 1:200.	Alexa Fluor 546-IgG
Nanog	Rabbit polyclonal antibody Nanog (ab21624,	Alexa Fluor 546-IgG

	Abcam). Dilution 1:200.	
hTERT (C-term)	Rabbit anti-human hTERT clone Y182 monoclonal antibody (MABE14, Millipore). Dilution 1:200.	Alexa Fluor 546-IgG